Research article

X-RAY SPECTROMETRY

Received: 18 December 2013 Revised: 23 June 2014 Accepted: 15 July 2014 Published online in Wiley Online Library

(wileyonlinelibrary.com) DOI 10.1002/xrs.2560

In vivo EDXRF scanning analysis of human nail

R. G. Figueroa,[a]* I. R. Chávez[a] and E. Bonzi[b]

This paper presents the results of a new technique for *in vivo* energy dispersive X-ray fluorescence (EDXRF) scan analysis, applied to human fingernails. The scan employs a specially designed EDXRF spectrometer, which allows a concentration profile of the elements detected in a human nail. In order to carry out this technique, a group of nail fragments taken from different people was analyzed. The elements S, Ca, Cu, Fe, Cu, Zn, and Pb were detected in most of the samples. A bidimensional (*x*, *y*) scan was also performed on a whole removed nail in which the 2D spatial distribution of the detected elements was observed. Significant differences in some of the detected elements were noted. Minimum time of average detection per element was determined, based on the EDXRF spectra of the nail fragment. The time required to obtain an *in vivo* element profile of a typical nail was thus determined, applying the same geometry and acquisition conditions for all cases. The dose that the person undergoing this type of EDXRF scan analysis would be exposed to was also determined. Exposure time does not exceed 15 s, and the calculated administered dose is in the surface nail region of 0.1 mGy/s. The results of this study demonstrate that it is possible to carry out an *in vivo* X-ray fluorescence scan analysis. This information may be used in different fields of medicine, such as nutrition and toxicology, and in other areas that establish a correlation between the concentration of the detected elements and certain diseases. Nail and hair are known to be 'accumulating tissues' unlike bodily fluids. In some aspects, nail analysis can be equal to a blood test.

Introduction

Fingernails are mainly made up of a fibrous protein, known as keratin, found in several epidermal formations such as feathers, horns, scales, nails, and hair.[1] Nails contain small quantities of trace elements such as Fe, Cu, and Zn.[2] The absence or excess of these elements has been associated with disorders or diseases, as well as nutritional factors. Dermatological studies show that changes in elements that nails are made up of and release are closely linked to people's health.[1] For example, Fe and Zn deficiencies have been detected in cystic fibrosis and asthma patients.[3] Significant alterations of Fe and Cu have been found in prostate, breast, thyroid, and lung cancer patients.[4] *In vivo* study of human nails is therefore important and relevant.

Studies of characterization of human nails removed from patients using the particle induced X-ray emission technique have been performed.[5] The results obtained using this technique show that elements such as Mg, Al, Si, P, S, Cl, K, Ca, Ti, Cr, Mn, Fe, Ni, Cu, Zn, Se, Br, Au, and Hg are present. Besides Hg, no toxic elements were found, e.g. As, Pb, and Cd, which would reflect any special anomaly in an individual's health. Other studies show the presence of heavy-contaminating elements in human bones, such as Pb.[6] With the energy dispersive X-ray fluorescence (EDXRF) technique, studies of element concentrations in organs and parts removed from living beings may be performed, as well as other investigations.[7] The technique has also been applied to *in vivo* analysis in different external parts of the human body, including knees, previous to the study of the dose delivered associated with these applications.[8]

Nails grow longitudinally, beginning in the proliferative matrix and extending toward its distal end. Their growth rate is 0.1 mm/day in adults[9]; thus, an entire nail takes approximately 150 days to grow. The individual's nutrition and toxicological history may be studied using the element composition of the nail at its various stages of growth.

Nails and hair are known to be 'accumulating tissues' compared with bodily fluids. In some aspects, nail analysis can be said to be equal to a blood test but involving the examination of a less labile source of information.[10] The time schedule is therefore much longer in these tissues. This allows us to observe the evolution of a disease through the fluorescent intensity profile or 2D image EDXRF of any chemical element as a biomarker along the line of nail growth. Hence, measurement in nails is especially important because the EDXRF technique is nondestructive, it can be performed *in vivo*, and given its features, it does not require any preparation, only that the nails are clean.

Different X-ray fluorescence (XRF) scan techniques have also been developed to obtain images or maps of elements in diverse biological and mineral samples.[11] These techniques generally use very small-sized samples. Other techniques that employ larger sample sizes have also been developed.[6]

A new large-area EDXRF scan technique that employs a robotic arm has recently captured bidimensional images of the spatial distribution of the chemical elements present in large-sized biological samples, such as human hands and jaw bones, chicken feet, rat liver, among others.[12] There are currently no known studies of *in vivo* scan analysis of nails that show the trace elements present in nails nor their spatial distribution.

An *in vivo* EDXRF scan technique for nails was analyzed and developed in this study according to the aforementioned information. This technique employs a specially designed EDXRF spectrometer that obtains a profile of the concentration of elements found along the length of a human nail, in addition to capturing bidimensional images of the chemical element distribution of the nail.

* *Correspondence to: Rodolfo Figueroa, Ciencias Físicas, Universidad de La Frontera. E-mail: rodolfo.figueroa@ufrontera.cl*

PACS numbers: 78.70.En, 07.85.Nc 87.59.-e 87.64.kd 87.53.Bn.

a *Department of Physical Sciences, Universidad de la Frontera, Temuco, Chile*

b *FaM.AF, Universidad Nacional de Córdoba, Córdoba, Argentina*

Methodology

In order to perform this study, a spectrometer composed of a mini tube X-ray (MTXR) Amptek 40 kV, 4 W, a digital pulse processor (DPP) with MCA (Amptek-PX4), a Silicon Drift Detector Si(Li) Amptex XR 100SDD, and a robotic arm was used. The detector and MTXR were placed at the end of the robotic arm at, at 45° and 90°, respectively, in relation to the sample's horizontal plane (*X*, *Y*). A finger holder was attached to the support table, which also holds a scan control device and DPP. These were both connected to the software that controls the mechanical scan system and the capture and processing of the XRF images. This software controls the step length, the acquisition time per point, the size of the 2D rectangular scan, the MTXR's voltage and current, and the DPP control. A photograph of the whole device is shown in Fig. 1.

The chemical elements, which have to be detected in nails by the EDXRF device, need to be established in advance. Thus, fixed-mode (nonscan) multi-element spectra of nail fragments, taken from a group of ten volunteers, were acquired (Universidad de la Frontera Scientific Ethics Committee, Approval Record number 86/2013), using a voltage of 40 (KeV), a current of 60 (μA) for the MTXR at a tube-sample distance of 15 (mm) and sample-detector distance of 10 mm. This was achieved by using geometry with the sample plane set at 90° in relation to the MTXR beam and 45° to the detector axis. The mode used in this case was fixed with an acquisition time of 180 s for each spectrum. Nail fragments were of various sizes and shapes of approximately 8 mm^2, cleaned with acetone and alcohol.

Then, in order to determine the spatial distribution (2D) of the elements present in a whole nail, an XRF image scan technique, developed by one of the authors,[13] was applied. Using the same voltage and current conditions as employed for the MTXR and the same geometry. With the intention of including the nail and the finger – fully and loosely – a scan covering 9 cm^2 (50 × 50 point-matrix) was performed with a 100-ms acquisition time per point (pixel), considering that nails have an area of approximately 270 mm^2 (17 × 16 mm^2).

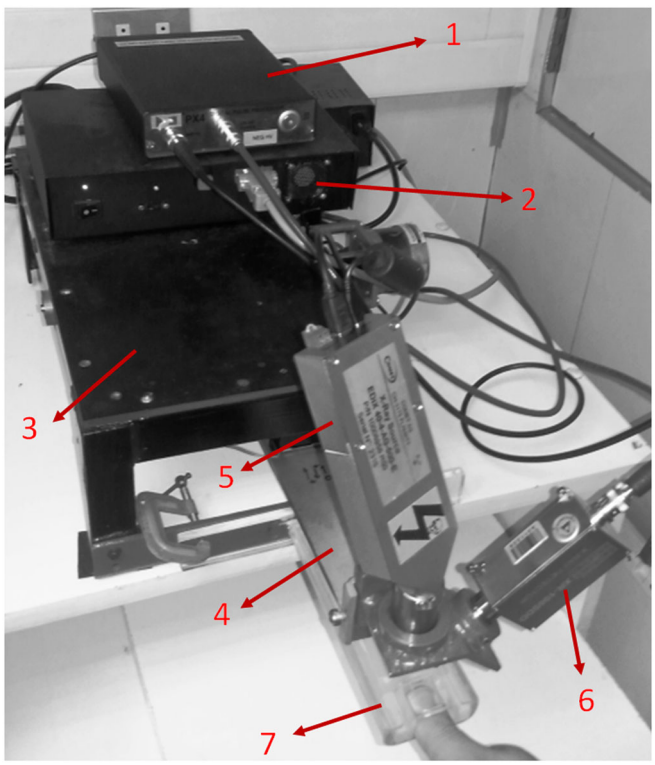

Figure 1. EDXRF scan spectrometer, showing its various components: (1) DPP multiprocessor, (2) scan control, (3) robotic arm support table, (4) robotic arm, (5) X-Ray mini tube, (6) SDD Si(Li) detector, and (7) finger holder.

The technique that was used practically suspends the sample in the air with a thin Plexiglas support, while the MTXR and the detector pass over the sample. When no scanning is carried out, the sensitivity depends on the EDXRF spectrometer, the setup, the matrix, and the elements that are present. Given that the nail is formed by curved homogeneous material, it is slightly higher in the center than at the edges (2–3 mm). In this study, the aforementioned text was not taken into account in the carrying out of the measurements.

Subsequently, the dose for an *in vivo* application was determined by a redundant pencil beam-type algorithm, supposing that the kinetic energy release in the medium absorption is the same as the dose.

Finally, the *in vivo* EDXRF technique was applied to two similar nails belonging to two *in vivo* volunteers, using the same voltage and current conditions along with an exposure time of 15 s. Two different software were used to obtain the *in vivo* EDXRF spectra. The first was developed by the authors for EDXRF image capture. The second software comes with the multiple-pulse DPP processors (the detector, amplifier, ADC, and MCA power supply from Amptek Inc.). The former software processes the bidimensional images, and the latter reports the energies of the fluorescence peaks, so as to then identify the elements present in the samples.

Dose calculation

The main components of the nail's matter (keratin) need to be identified so as to determine the dose that can be administered to a patient when undergoing a human nail *in vivo* EDXRF scan analysis; the mass attenuation coefficients (μ/ρ) of the keratin in the incident ray must be determined, including the rest of the exposed matter, muscle, bone, and skin in the calculation, using Eqn (1).

$$u_M(E) = \frac{u}{\rho} = \frac{1}{\rho}\sum_{i=1}^{n} C_i \cdot \mu_i(E) \quad \left[\mathrm{cm}^2/\mathrm{g}\right] \tag{1}$$

Where C_i is the mass elemental concentration of the element *i*, $\mu_i(E)$ is the linear attenuation of element *i* to the energy *E*, and ρ is the density of the matter (keratin).

The incident spectrum of the X-ray tube at 15 mm must also be known (Fig. 2) and must be considered in the algorithm used to calculate the dose. It should be noted that the enormous peak at low energy corresponds to the L line of the silver tube, which appears only at short distance in air; the peak practically disappears at distances greater than 10 cm of air. However, it must be considered for dose calculation because it has effects on the surface level, and the measurements are performed at short distance. This spectrum was determined using the minimum current in order to avoid saturation and was corrected for dead time losses.

In order to calculate the dose (*D*), the pencil beam method was employed with narrow beam geometry, along with an algorithm developed by one of the authors. This was considered in the calculation of the dose in Eqn (2).

$$D(x) = \frac{\Delta E}{\Delta m} = \sum_{n=1}^{n_{\max}} N_0(E_i)\ E_i \left(\frac{\left(1 - e^{-\mu(E_i)\ x}\right)}{\rho\ A\ \Delta x}\right) \quad [\mathrm{J/Kg}] \tag{2}$$

Where,
E_i : ith energy of the incident spectrum.
$N_o(E_i)$: number of photons of energy E_i.

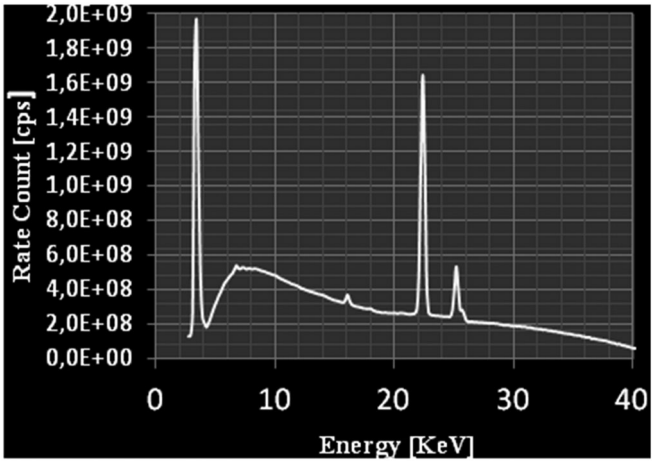

Figure 2. X-ray tube incident spectrum at a short distance from its output window.

$\mu(E_i)$: linear attenuation coefficient of the material to the ith energy.
x : depth in the material.
ρ: mass density of the material to estimate i esima energy.
A : irradiated area section.
Δx : irradiated area section thickness considered.

The results were compared with those obtained in a previous study in which similar calculations were used, as well as a Monte Carlo simulation (PENELOPE code)[14] plus measurements near the finger nail surface using a small ionization chamber RADCAL 10X6-3CT.

Results and discussion

Removed nail fragments: fixed mode

Fluorescence peaks can be seen in S, Cl, Ar, Ca, Ti, Cr, Fe, Cu, Zn, and Pb. Elements were identified by the emissions of K_α and K_β and in some cases L_α. Table 1 shows the net areas under the fluorescence peaks of the elements with the highest number of counts per second, detected by our spectrometer. The information was taken from the Amtek Inc. program. This information makes it possible to graph the net areas according to the individuals. These results are in net counts under the peak and represent the fluorescence intensity associated with each element detected.

Figure 3 shows the EDXRF spectra corresponding to fragments of nails from ten volunteers. The presence of minority elements in the nail can be clearly seen (Ti, Cu, Fe, Zn, Pb). These vary from individual to individual as does the quantity of each element present in each nail. For example, significant differences in Zn levels in different individuals were observed, seen throughout greater areas under the fluorescence peaks. Pb is an element that is not present in all individuals or is present in quantities that were not detectable by our spectrometer but is present in greater amounts in other individuals. The quantity of Zn, Cu, and Fe differs significantly from person to person. In some cases, the amount of Cu and Zn doubles from one individual to the next. Other authors found similar results,[5] and[15] at this stage of the investigation, the minimum detectable has not been provided yet. It is expected to be developed in a second stage. In any case, the minimum detectable will vary because it depends on several parameters, including the recording time per pixel.

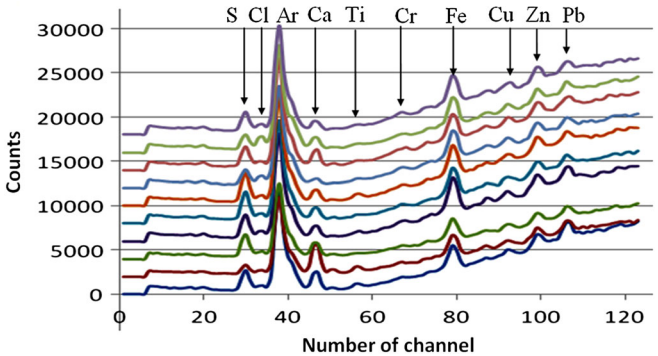

Figure 3. Spectra of ten nail fragments from university students. Number of net counts according to the number of the detector's canals.

Table 1. Net areas of the fluorescence peaks for each element of each analyzed nail

Element	Nail 1	Nail 2	Nail 3	Nail 4	Nail 5
Pb	0	1490 ± 40	2020 ± 50	1760 ± 40	1560 ± 40
Ti	1320 ± 40	530 ± 220	730 ± 30	3470 ± 60	LDL
Fe	2480 ± 50	2090 ± 50	2470 ± 50	4400 ± 70	3520 ± 60
Cu	3540 ± 60	5630 ± 80	5340 ± 70	5060 ± 70	7670 ± 90
Zn	5570 ± 80	3670 ± 60	4530 ± 70	5990 ± 80	5530 ± 70
Ca	4290 ± 70	LDL	6200 ± 80	6060 ± 80	4830 ± 70
Element	Nail 6	Nail 7	Nail 8	Nail 9	Nail 10
Pb	LDL	1350 ± 40	1080 ± 30	2000 ± 50	1510 ± 40
Ti	690 ± 30	LDL	LDL	LDL	LDL
Fe	2860 ± 50	1990 ± 50	1500 ± 40	2160 ± 50	1990 ± 50
Cu	5930 ± 80	4960 ± 70	4910 ± 70	5560 ± 80	4690 ± 70
Zn	3600 ± 60	4550 ± 70	4570 ± 70	4560 ± 70	4670 ± 70
Ca	LDL	7900 ± 90	4700 ± 70	6200 ± 80	7250 ± 90
S	12000 ± 100	14200 ± 100	9040 ± 90	13400 ± 100	13800 ± 100

LDL, low detection limit.
These results are in total net counts under the peak.

Ti is an element that is present in approximately 50% of the analyzed nails. This coincides with the results obtained by other authors.[5]

The methodology and technique employed in this study generally represent the ability to discriminate and differentiate the presence and concentration of elements among individuals.

Whole nail using bidimensional scan

Figure 4 shows EDXRF scans of a nail removed from a person, including its different substrates: acrylic (in green and greater background above), whole nail in air (violet, in the middle), and longitudinal segment of the nail (light blue, below).

The fluorescence peaks of S, Ar, Ca, Cu, Fe, Zn, and Pb are seen in the three spectra. There is a minimal difference in the matrix, which indicates that it is possible to perform a short-interval longitudinal scan of the nail without losing any relevant information about its composition. This can be seen in the light blue spectrum, which only differs from the others in its lesser intensity and background (matrix + nail). With the purpose of reducing the presence of unwanted setup element contributions, full scans were performed in air on a whole extracted nail. Furthermore, when working *in vivo*, the beam was collimated to a narrow beam of 1.5 mm effective size in diameter on the surface of the nail, so it would impact only the central part of the nail, thus minimizing the potential contributions of setup elements.

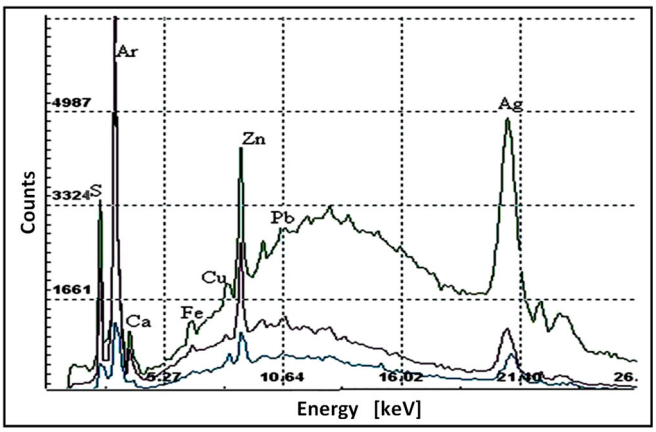

Figure 4. X-ray fluorescence spectra of a nail removed from a patient. Green spectrum, whole nail with PMMA base/background; red spectrum, whole nail in air; light blue spectrum, longitudinal scan of 16 mm^2 area with an exposure time less than 20 s (set times each).

The bidimensional distributions of the six elements detected in the removed nail were obtained using a specially designed EDXRF scan program.[16] These distributions were edited using the Image J program, which is shown in Fig. 5. The images were based upon the percentage analysis of net areas in relation to the total area of the fluorescence peaks of each element so as to subtract the input of the background matrix at each intensity. Hence, the greater 'luminosity' in each image shows, approximately, the net presence of each element in the nail (Fig. 5).

These results show the relevance of making such longitudinal scan, because the elements detected appear to have a fixed position within the nail matrix, for the time elapsed during the measurement. Thus, it displays a snapshot of the past 3 months with lot of detailed information. However, despite the fact that this research does not intend to decode that information, it is important to mention that a similar analysis is not possible through blood tests, biopsies, or other types of fluids.

Most of the elements have an irregular distribution, with higher or lower periods of presence within the whole nail. For example, Fe and Cu appear only slightly in the center of the nail but are present at a higher concentration at the nail's proximal end. Zn and Ca also present a higher concentration at the distal end of the nail and a weak concentration in the rest of it. Pb presents a greater concentration at both distal and proximal ends of the nail. However, S is distributed almost uniformly along the entire nail, which coincides with the fact that S is one of the components of keratin, which is the nail matrix.

Dose calculation

Figure 6 shows the graph of the dose depending on the depth for the irradiated finger (heterogeneous sample). The average dose rate calculated by Eqn (2) was 0.03 mGy/s, and the dose rate extrapolated

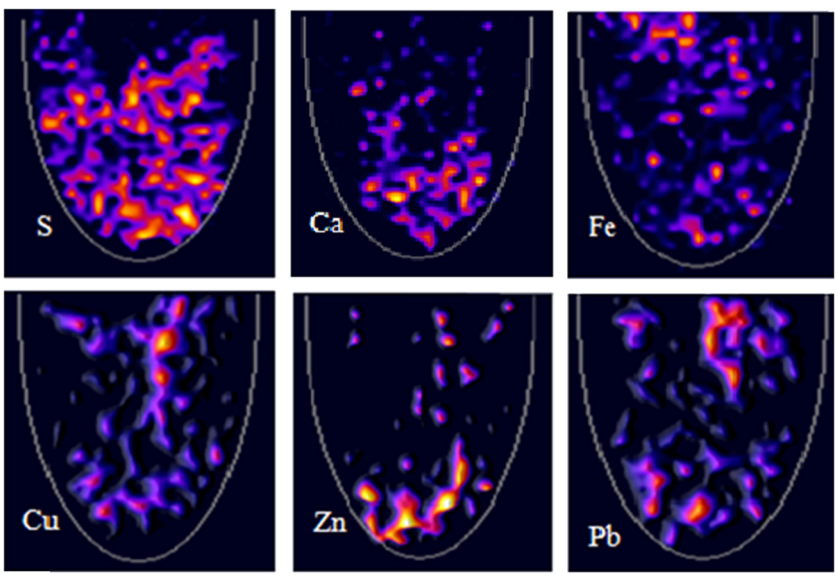

Figure 5. EDXRF images showing the bidimensional distribution of sulfur (S), calcium (Ca), iron (Fe), copper (Cu), zinc (Zn), and lead (Pb) in whole nail.

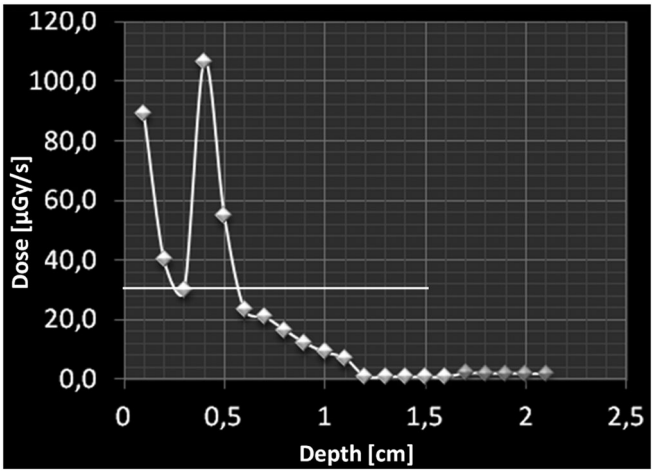

Figure 6. Depth dose rate calculate with MTXR at 40KV/60 µA, collimator 2 mm, MTXR-nail distance 1.5 cm. Horizontal line gave the average rate dose equal 30 µGy/s.

to the surface was approximately 0.10 mGy/s. Dose rate peak equals 0.11 mGy/s at 4 mm depth, because of the presence of bone material, which has a much greater attenuation coefficient than that of soft tissues and thus, a greater dose delivery in the bone. Therefore, the accumulated dose on the surface for an application of 15 s equals 1.50 mGy, and the mean dose equals 0.46 mGy.

The latter results are consistent with those obtained using Monte Carlo PENELOPE code[8] and with experimental measurements achieved with RADCAL 10X6-3CT camera, which gave an accumulated dose value of 1.48 mGy ± 0.05 considering the same measurement time than that used for calculation. Therefore, it is possible to perform an *in vivo* analysis of human nails, as the dose administered to patients is within the range established for diagnostic exams.[17]

In vivo EDXRF

In vivo spectra

The graph shown in Fig. 7 shows the fluorescence spectra of the longitudinal scans of the three analyzed nails (one removed nail and two *in vivo*).

Longitudinal images: mono element profiles

The images displayed in Fig. 8 correspond to the lineal distribution of each element detected in removed nail (red), subject 1 *in vivo* nail (blue), and subject 2 *in vivo* nail (green). The dark color represents a low presence of the element, and the white shows a high presence of the element in that section of the nail. The red line represents the distal end of the nail. Scan: distal end on the left and proximal end on the right.

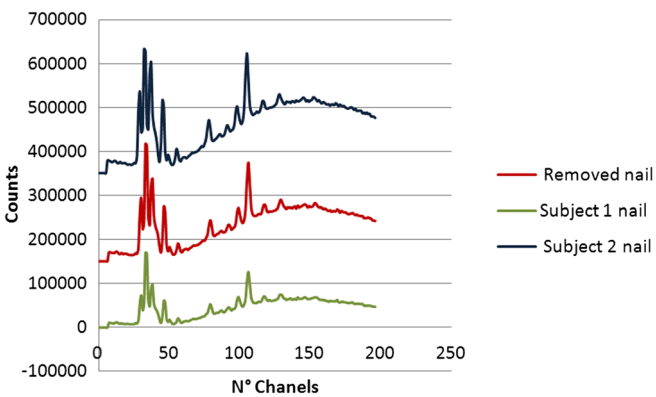

Figure 7. EDXRF spectra of the three nails. Removed nail (red spectrum), subject nail 1(green spectrum), and subject nail 2(blue spectrum).

When the spectrum of the removed nail was compared with the two *in vivo* spectra in Fig. 8, a similar element composition is evident, with slight variations between element intensities. The detected elements (sulfur, chlorine, calcium, nickel, iron, copper, zinc, and lead) are present in each of the nails in various concentrations and spatial distributions unique to each element. This is shown in the mono element longitudinal profile images (Fig. 9). For example, a distribution of S with certain variability was observed, despite the fact that this element is identified as a component of the nail matrix. The detected elements that are shown in Fig. 9, such as Ni, Fe and Cu, Zn and Pb, at first glance present irregular distribution, which accounts for the variations of the concentrations of each element during the growth period of the nail. Error bars are set upon the statistical errors associated with each measurement peak area. Ca hardly makes an appearance in any of the three nails, or its concentration was not enough to be detected with this methodology, given its short exposure time, except the distal end where its concentration increases in all three cases, although we have no explanation for this particular fact.

The detected elements coincide with those found by other authors,[5] although this was not the case with their bidimensional distribution. There is a report concerning the homogeneous distributions of Ca, P, Na, Mg, Rb, Br, Sr, and Se along the nail matrix, and it does not show distributions of heavy elements.[15]

Detailed variation of the intensities along the length of the nails is presented in the following text.

In vivo longitudinal profiles

This analysis may be corroborated to a greater extent with the graphs of the normalized net counts at Argon's peak, according to the number of steps corresponding to each bidimensional image of the detected elements (Fig. 9). Argon peak appears because the analysis was performed in the presence of air, and Ar is a component of it.

Assuming that the matrixes of the nails that were analyzed *in vivo* are similar, it can be observed that Zn is present at a higher concentration in subject 1's nail compared with the other two nails and likewise at the distal end of subject 1's nail.

Cu is distributed very irregularly along the growth line of the nail, which moderately accounts for the variations in its concentration along the growth line. A greater concentration of Cu in subject 1's nail is also visible in comparison with the other nails.

In the case of Fe, subject 1's nail has a low concentration of the element at the proximal end and increases in areas near the distal end. However, subject 2 has a greater concentration of Fe at the proximal end, which rises considerably near the distal edge. This helps us determine that the used methodology permits the discrimination of the differences in concentration from one individual to the next. In addition, it allows us to discriminate between the differences of concentration in different positions with regard to the direction in which the nail grows. We can observe concentration differences through changes in fluorescence intensity, but for now, quantifying it is not the purpose of this research.

The information obtained from the removed nail, based on the bidimensional image and the graphs of each element, was entirely reproducible and comparable with the *in vivo* nails. Thus, it is

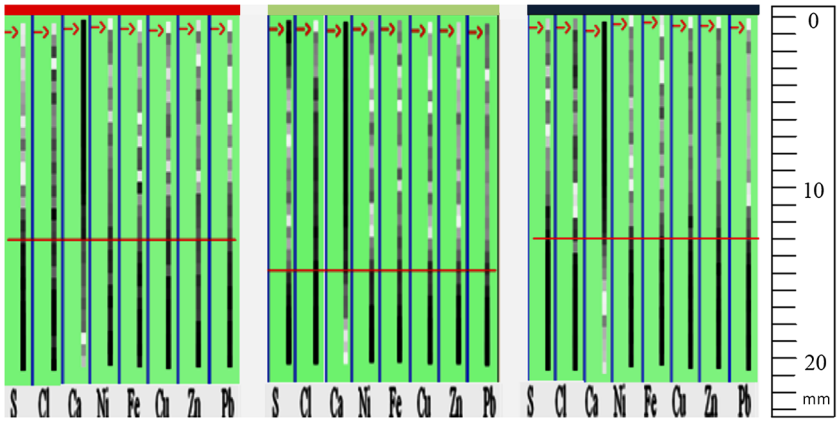

Figure 8. Fluorescence intensity profiles along the entire nail (linear images) of present elements detected by the EDXRF system, from left to right: S, Cl, Ca, Ni, Fe, Cu, Zn, and Pb. The red line represents the distal end of the nail and the lateral rule graduated in (mm). Removed nail (red mark), subject nail 1(green mark), and subject nail 2(blue mark).

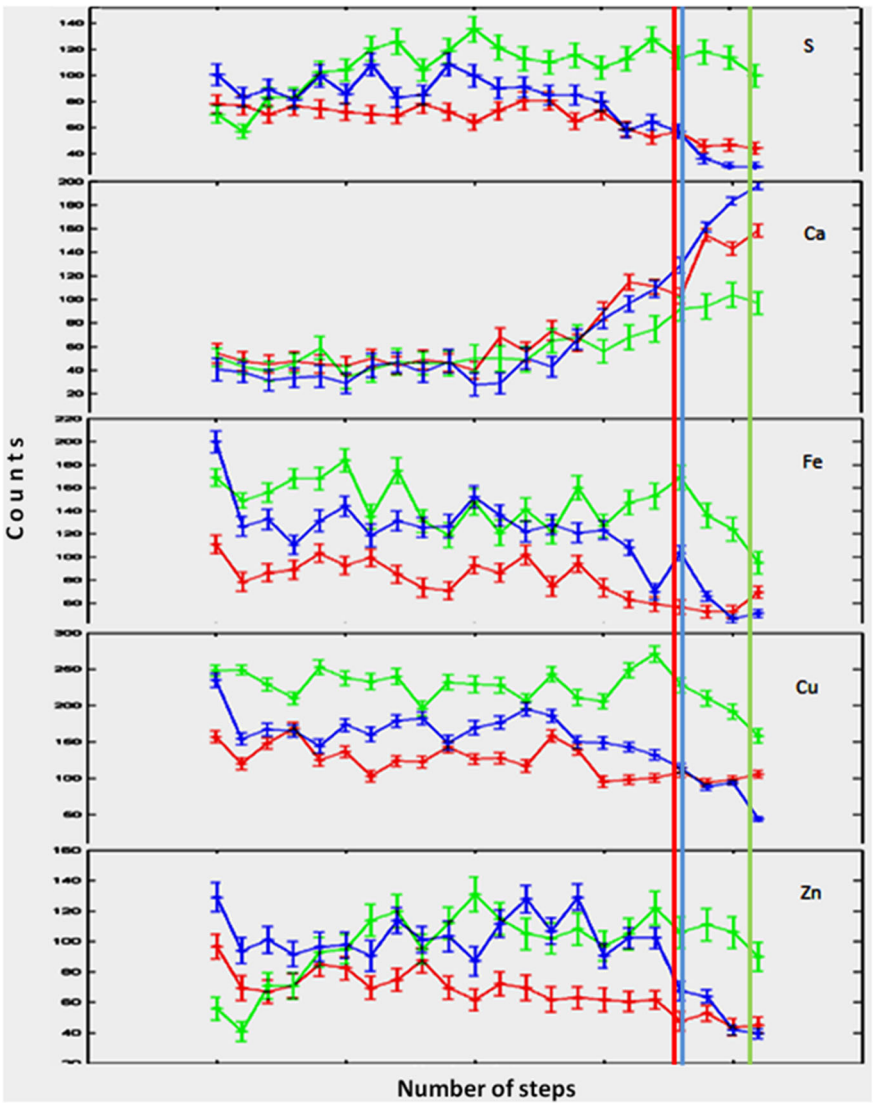

Figure 9. Comparative intensities K_α peaks of S, Ca, Fe, Cu, and Zn, with their error bars. Removed nail (red curve), subject 1 nail (green curve), and subject 2 nail (blue curve). Vertical lines show the end of the scan for each nail, using the same color criteria.

inferred that it is possible to perform *in vivo* analyses employing this methodology, and therefore, contamination risks are minimal, because the analysis is performed on clean fingernails.

The technique and methodology proposed in this study are applicable *in vivo* because of the low dose that the individual receives when irradiated for a few seconds. It also analyzes the concentration and spatial distribution of each element that is present in the nail and its evolution over time.

In our analysis, we have discarded the presence of elements below the nail, soft tissues, because they have not been reported in the literature and because of the low energy of the detected fluorescent X-ray. Furthermore, we have reference elements appearing *in vivo* samples, which are the same as those of the extracted nail.

In general, reproducibility of the technique is the usual for any EDXRF technique; the only difference is the spectrometer scan on the sample. Consequently, reproducibility of this technique depends mainly on the mechanical characteristics of the scanning device. In our case, we can establish reproducibility at around 100% for all cases, within the period of analysis of this experiment.

Other analytical techniques such as particle induced X-ray emission or ASS cannot be compared with this technique, because it is not possible to scan them. Furthermore, the purpose of this study was to demonstrate the feasibility of this technique and not be compared with a gold standard.

Conclusions

The results show the following:

Using an EDXRF scan spectrometer set to fixed mode, the presence of S, Cl, Ca, Ti, Cr, Fe, Cu, Zn, and Pb was detected in a group of nail fragments taken from ten volunteers. A similar spectral XRF profile was noted among the ten, with relative differences in the areas associated with each of the elements. One may observe that, spectrally, there are significant element differences between one individual and another. This could set a type of characteristic mark between one individual and the next.

With the EDXRF spectrometer set to scan mode, the 2D (bidimensional) distribution of the elements S, Ca, Fe, Cu, Zn, and Pb in a whole removed nail was determined. Significant spatial differences of the elements were observed.

In vivo EDXRF scan applications, using the same device, were performed on the thumb nails of two volunteers. Profiles of the mono element distribution intensities of approximately 20 mm along the length of the nails' direction of growth, specifically in the central area, were achieved in both samples. The *in vivo* profiles were acquired in 15 s per finger. There are significant differences, longitudinally, between the detected elements.

The determined dose for this type of *in vivo* applications was of around 1.6 mGy and concurs with that calculated in a previous study. It can be inferred that it was possible to apply this EDXRF scan methodology on people *in vivo* at a minimum risk to the individuals.

The technique proposed in this study was the first step in performing *in vivo* element scan analysis research on nails. This could contribute toward the diagnosis of some pathologies and intoxications that can be detected because of the chemical elements that are identified in nails and to the development of a prototype for clinical use.

Therefore, measured chemical element in nails are especially important because the EDXRF technique is nondestructive, can be performed *in vivo*, and, given its features, it requires practically no preparation.

Acknowledgements

This study was supported by Chile's FONDECYT through Proyecto 1080306 and by the Masters in Medical Physics Program of the Department of Physical Sciences of the Universidad de La Frontera in Temuco, Chile.

References

[1] A. Tosti, N. Cameli, B. Piraccini, P. Fanti, J. Ortonne. *J. Am. Acad. Dermatol.* **1994**, *31*(2), 193–196.
[2] M. Uo, K. Asakura, E. Watanabe, I. Hayashi, T. Yanagi, H. Shimizu, F. Watari. *Nano Biomed.* **2010**, *2*(2), 103–106.
[3] M. Katsikini, F. Pinakidou, E. Mavromati, E. C. Paloura, D. Gioulekas, D. Grolimund. *Nucl. Instrum. Methods Phys. Res., Sect. B* **2010**, *268*(3–4), 420–424.
[4] A. Gupte, R. J. Mumper. *Cancer Treat. Rev.* **2009**, *35*(1), 32–46. doi:10.1016/j.ctrv.2008.07.004.
[5] S. O. Olabanji, O. A. Ajose, N. O. Makinde, M. C. Buoso, D. Ceccato, M. De Poli, G. Moschini. *Nucl. Instrum. Methods Phys. Res., Sect. B* **2005**, *240*(4), 895–907. doi:10.1016/j.nimb.2005.06.206.
[6] D. E. B. Fleming, M. R. Gherase, K. M. Alexander. *X-Ray Spectrom.* **2011**, *40*(5), 343–347. doi:10.1002/xrs.1358.
[7] J. Börjesson, M. Isaksson, S. Mattsson. *Acta Diabetol.* **2003**, *40*(Suppl 1), S39–44. doi:10.1007/s00592-003-0024-z.
[8] R. Figueroa, E. Lozano, M. Valente. *Rev. Mex. Fis.* **2013**, *59*(4), 339–342.
[9] Cristina Serrano Falcóna y Salvio Serrano Ortega, Conducta ante una melanoniquia longitudinal de la uña, a.Área de Dermatología. CHARE Guadix. EPHP. Granada. España.bCátedra de Dermatología. Facultad de Medicina. Universidad de Granada.Granada. España, **2013**.
[10] D. A. R. de Berker, and R. Baran, Science of the nail apparatus, in Baran & Dawber's Diseases of the Nails and Their Management, 4th edn, Blackwell Publishing Ltd., Oxford, UK, **2012**, doi: 10.1002/9781118286715.ch1.
[11] R. Alberti, C. Fiorini, C. Guazzoni, T. Klatka, A. Longoni. *Nucl. Instrum. Methods Phys. Res., Sect. A* **2007**, *580*(2), 1004–1007.
[12] R. G. Figueroa, E. Lozano, G. Bongiovanni. *Rev. Mex. Fis.* **2013**, *59*(4), 292–295.
[13] R. G. Figueroa, E. Lozano, M. A. Flores. *Int. J. Insect Morphol.* **2011**, *29*(3), 1000–1006.
[14] R. G. Figueroa, E. Lozano, M. Valente, *Rev. Mex. Fis.* **2013**, *59*(*4*), 339–342.
[15] S. Joon-Tae, S. Hyunchang. *J. Korean Phys. Soc.* **2010**, *57*(5), 1285. doi:10.3938/jkps.57.1285.
[16] C. A. Pineda-Vargas, J. A. Mars, D. Gihwala. *Nucl. Instrum. Methods Phys. Res., Sect. B* **2012**, *273*, 153–156. doi:10.1016/j.nimb.2011.07.063.
[17] IAEA, TECDOC 1646, Establecimiento de Niveles Orientativos en Radiografía General y Mamografía, Reporte del Proyecto Coordinado ARCAL LXXV- IAEA RLA/9/048 Organismo Internacional de Energía Atómica VIENA, **2010**.